(1)

OSU

The Ohio State University

AN EFFICIENT GEODESIC PATH SOLUTION FOR PROLATE SPHEROIDS

by

Nan Wang and W.D. Burnside

AD A115063

The Ohio State University

ElectroScience Laboratory

Department of Electrical Engineering
Columbus, Ohio 43212

QUARTERLY REPORT 711305-2

July 1979

Contract N00019-78-C-0524

Department of the Navy
Naval Air Systems Command
Washington, D.C. 20361

NOTICES

CONTENTS

SECURITY CLASSIFICATION OF THIS PAGE (When Data Entered)

REPORT DOCUMENTATION PAGE		READ INSTRUCTIONS BEFORE COMPLETING FORM
1. REPORT NUMBER	2. GOVT ACCESSION NO. AD-A115 063	3. RECIPIENT'S CATALOG NUMBER
4. TITLE (and Subtitle) AN EFFICIENT GEODESIC PATH SOLUTION FOR PROLATE SPHEROIDS		5. TYPE OF REPORT & PERIOD COVERED Quarterly Report
		6. PERFORMING ORG. REPORT NUMBER ESL 711305-2
7. AUTHOR(s) Nan Wang and W. D. Burnside		8. CONTRACT OR GRANT NUMBER(s) Contract N00019-78-C-0524
9. PERFORMING ORGANIZATION NAME AND ADDRESS The Ohio State University ElectroScience Laboratory, Department of Electrical Engineering Columbus, Ohio 43212		10. PROGRAM ELEMENT, PROJECT, TASK AREA & WORK UNIT NUMBERS
11. CONTROLLING OFFICE NAME AND ADDRESS Department of the Navy Naval Air Systems Command Washington, D.C. 20361		12. REPORT DATE July 1979
		13. NUMBER OF PAGES 20
14. MONITORING AGENCY NAME & ADDRESS(if different from Controlling Office)		15. SECURITY CLASS. (of this report) Unclassified
		15a. DECLASSIFICATION DOWNGRADING SCHEDULE

16. DISTRIBUTION STATEMENT (of this Report)

APPROVED FOR PUBLIC RELEASE DISTRIBUTION UNLIMITED

17. DISTRIBUTION STATEMENT (of the abstract entered in Block 20, if different from Report)

18. SUPPLEMENTARY NOTES

19. KEY WORDS (Continue on reverse side if necessary and identify by block number)

Airborne antenna
Geometrical theory of diffraction
Electromagnetic radiation
High frequency solution
Geodesic path
General convex body of revolution
Spheroid

20. ABSTRACT (Continue on reverse side if necessary and identify by block number)

> A major task in the application of the geometrical theory of diffraction (GTD) to the problem of electromagnetic radiation from a general convex surface is to determine the unique geodesic path that starting from the source location traverses the surface and has a tangent at some point along the path which points in the desired radiation direction. In this report a numerically efficient and accurate scheme has been developed for solving this problem in the case of a general convex surface of revolution.

DD FORM 1 JAN 73 1473 EDITION OF 1 NOV 65 IS OBSOLETE

SECURITY CLASSIFICATION OF THIS PAGE (When Data Entered)

20.

The surface of revolution is of interest in that it provides an analytic model for the aircraft fuselage structure. A computer program is also developed to solve the governing nonlinear equation using the secant method for iteration. This method is proved to be simple and converges to the accurate results in just a few steps. Numerical results for the family of geodesic curves are also presented for the cases of sphere, prolate spheroid and cylinder.

I. INTRODUCTION

For an airborne antenna mounted on the fuselage of an arbitrary aircraft near the extreme top or bottom, the fuselage shape has the dominant effect on the resulting radiation pattern. The wings and other flat plate structures can have strong effects in certain sectors of the pattern but they are not as dominant as the fuselage especially when the complete volumetric pattern is concerned. Previous analyses [1,2] for the airborne antenna performance employed a profile cylinder model for the evaluation of the radiation pattern in and near the elevation plane; whereas, a cross-section cylinder model was used for the pattern calculation elsewhere. Thus for pattern calculations off the principal planes, a two-cylinder model [2] was employed for the analysis. Although this two-cylinder model provides a useful means to obtain satisfactory results for the volumetric pattern calculations, there are some problems encountered in the nose and tail sectors of the pattern. This results from the fact that the geodesics (ray paths) used in the two-cylinder model does not travel on the true three-dimensional surface of the fuselage. As a consequence, the unit normal and binormal vectors of the geodesic for the two cylinders do not vary continuously on the surface. This leads to erroneous results and discontinuities in the calculated patterns. Due to the above mentioned difficulties, it is apparent that an improved three-dimensional model is needed for the fuselage structure. An attempt has been made previously to model the fuselage as a body of revolution [1], and good results were obtained for an antenna radiating from a prolate spheroid. According to the geometrical theory of diffraction (GTD) analysis, an antenna located on the surface launches a ray which propagates along the geodesic path on the surface and continuously sheds electromagnetic energy in its tangent direction. A typical ray picture for an antenna radiating from a surface of revolution is shown in Fig. 1, in which a ray launches from S, and traverses along the geodesic path to the shedding point Q, and then propagates along the tangent direction at Q in the observation direction $\hat{r}(\theta_r,\phi_r)$. Thus a major task in the analysis is to determine the unique geodesic path $\hat{SQ}$ associated with a given desired radiation direction $\hat{r}(\theta_r,\phi_r)$. The previous numerical technique [1] was not very efficient in that a tedious interpolation procedure was employed to determine the unique geodesic path whose tangent points in the desired radiation direction.

In this report, a three-dimensional model for the fuselage shape, namely, a body of revolution model, is re-examined and an efficient method is developed to find the unique geodesic corresponding to the desired radiation direction. This method is described in detail in the following section.

II. GEODESICS ON A BODY OF REVOLUTION

Consider a body of revolution with the parametric representation of its surface given as follows:

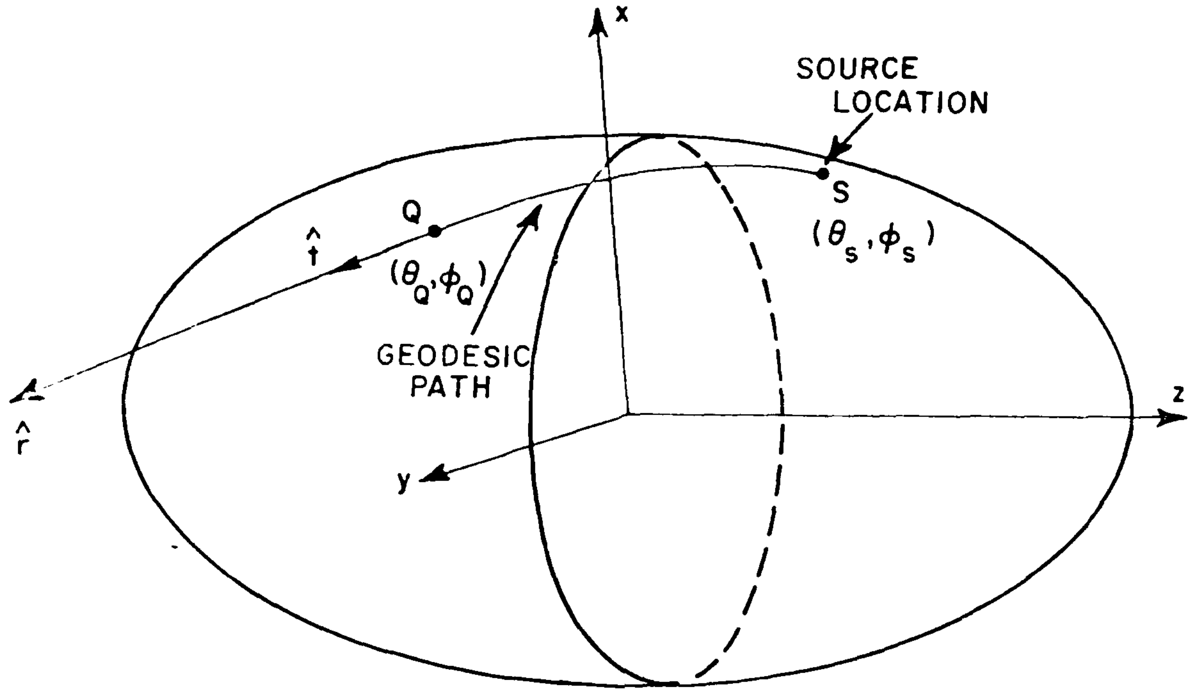

Figure 1. An antenna radiating from a general convex surface.

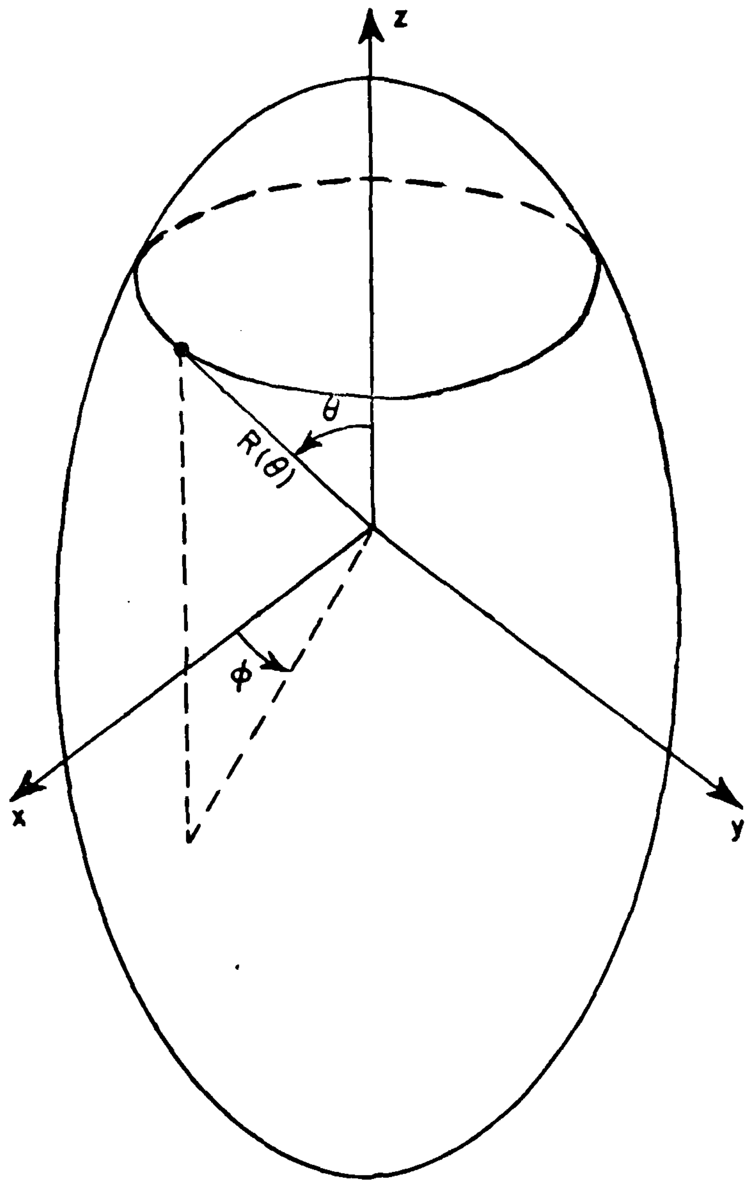

Figure 2. A surface of revolution and the associated coordinate system.

$$\vec{X}(\theta,\phi) = R\sin\theta\cos\phi\hat{x} + R\sin\theta\sin\phi\hat{y} + R\cos\theta\hat{z} \qquad (1)$$

where (R,θ,ϕ) is the usual spherical coordinate system, and R is a function of theta i.e., $R=R(\theta)$. The surface is illustrated in Fig. 2.

It can be shown that the arc length between two points on the body of revolution can be expressed[3] as

$$\ell = \int [R'^2 + R^2 + R^2\sin^2\theta(\phi')^2]^{1/2} d\theta \qquad (2)$$

in which R' and ϕ' are the derivatives with respect to the variable θ. According to the calculus of variation[4], the arc length with minimum distance between the two points (the geodesic) should satisfy the following constraint:

$$\frac{R^2\sin^2\theta\phi'}{[R'^2+R^2+R^2\sin^2\theta(\phi')^2]^{1/2}} = \text{constant} = A. \qquad (3)$$

Equation (3) can be rearranged and one obtains the following expression for the geodesic on a body of revolution:

$$\phi' = A\left|\frac{(R')^2+R^2}{R^2\sin^2\theta(R^2\sin^2\theta-A^2)}\right|^{1/2} \qquad (4a)$$

or

$$\phi = \phi_s + A\int_{\theta_s}^{\theta}\left[\frac{(R')^2+R^2}{R^2\sin^2\theta(R^2\sin^2\theta-A^2)}\right]^{1/2} d\theta \qquad (4b)$$

In the above equation (θ_s,ϕ_s) is the starting location of the geodesic, and the constant A is related to the starting direction $\phi'|_s$ at the starting location through Equation (3).

As an example, let us consider the prolate spheroid with major and minor axes "a" and "c" as shown in Fig. 3. For the prolate spheroid shown in Fig. 3, it is easy to show that

$$R(\theta) = \frac{ac}{(a^2\cos^2\theta+c^2\sin^2\theta)^{1/2}} \qquad (5)$$

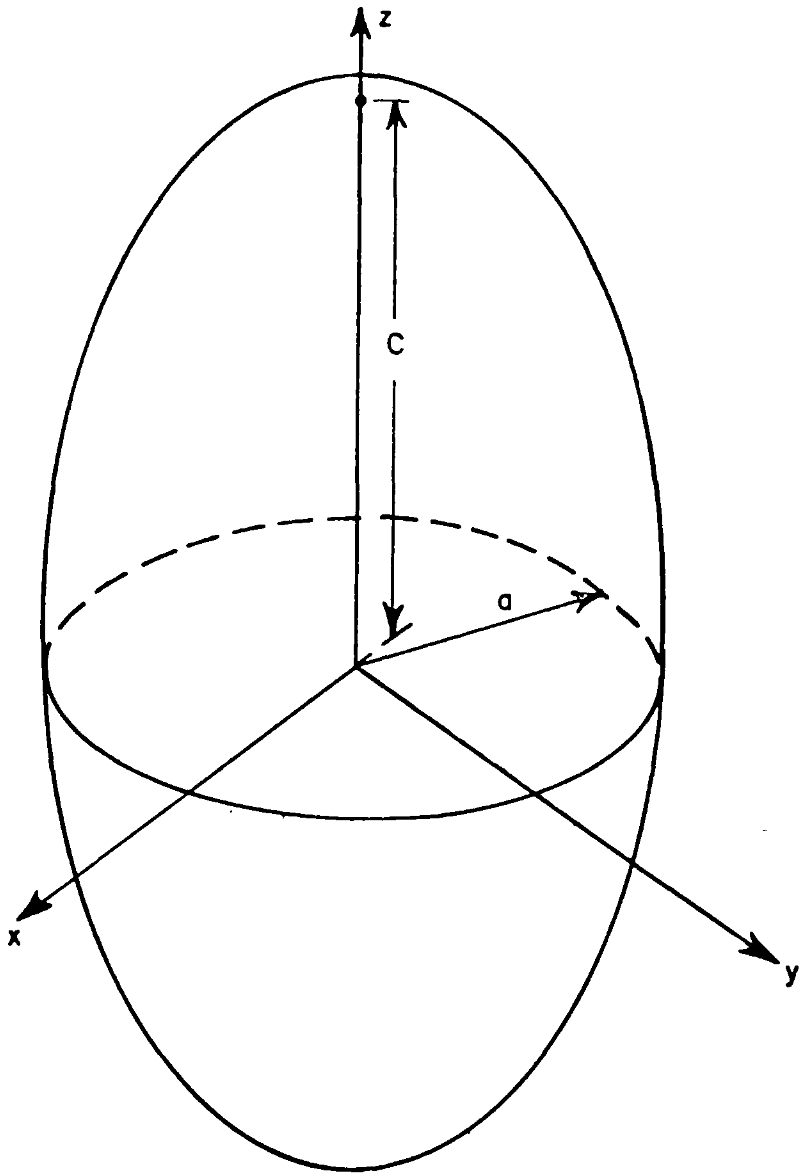

Figure 3. A prolate spheroid with major and minor axes a and c.

and

$$R' = \frac{dR}{d\theta} = \frac{-ac\ \sin\theta\cos\theta(c^2-a^2)}{(a^2\cos^2\theta+c^2\sin^2\theta)^{3/2}} \quad . \tag{6}$$

By specifying θ_s, ϕ_s and $\phi'|_s$ at the starting position on the prolate spheroid, Equations (4), (5) and (6) can be employed to generate a family of geodesic curves on the spheroid. It is convenient to introduce a new variable ω_s such that

$$\phi'|_s = -\cot\omega_s \quad . \tag{7}$$

Substituting Equation (7) into (3), one obtains

$$A = \left. \frac{R^2\sin^2\theta(-\cot\omega_s)}{\sqrt{(R')^2+R^2+R^2\sin^2\theta\cot^2\omega_s}} \right|_s \tag{8}$$

Notice that for ω_s equal to 90° or 270°, the geodesic equation reduces to $\phi=\phi_s$, i.e., the geodesic is the generating curve of the body of revolution, the meridians. It should also be noted that Equation (4) does not predict the geodesic circle, the Equator, $\theta=90^\circ$ as a result of choosing Equation (4) as the representation of the geodesic. Now let us examine some numerically computed geodesic paths. In Fig. 4 the geodesic curves for a starting location $\theta_s=90^\circ, \phi_s=0^\circ$ on a 2x4 prolate spheroid are plotted. For a given staring direction ω_s, the geodesic path is specified by a set of points on the spheroid surface with θ and ϕ being the position parameters. In Figs. 5 and 6, geodesic curves are shown for two different starting locations, ($\theta_s=60^\circ, \phi_s=0^\circ$) and ($\theta_s=30^\circ, \phi_s=0^\circ$), respectively. Since the aircraft fuselage usually resembles a long cylindrical structure, Fig. 7 shows the geodesic curves for a 2x100 prolate spheroid. It is interesting to notice that the geodesic curves for the 2x4 and 2x100 spheroid are very similar to each other. Finally, the geodesic for a sphere is shown in Fig. 8.

Now that the geodesic paths are known for the surface of revolution, the radiation direction along the geodesic must be found for each path. Recall that the parametric representation of the geodesic on a surface of revolution is

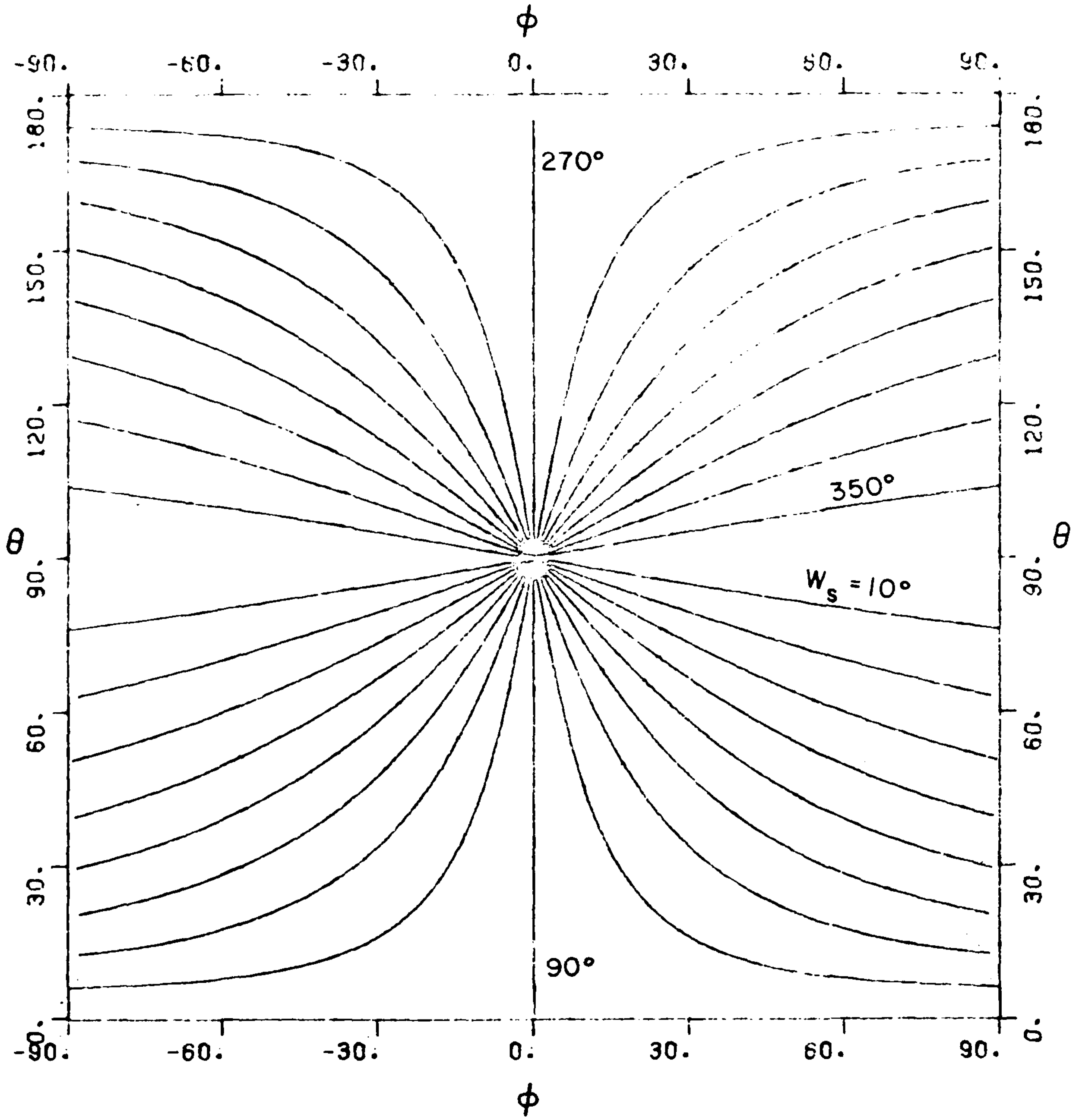

Figure 4. Geodesic paths on a 2x4 prolate spheroid. (θ_s=90^0, ϕ_s=0^0).

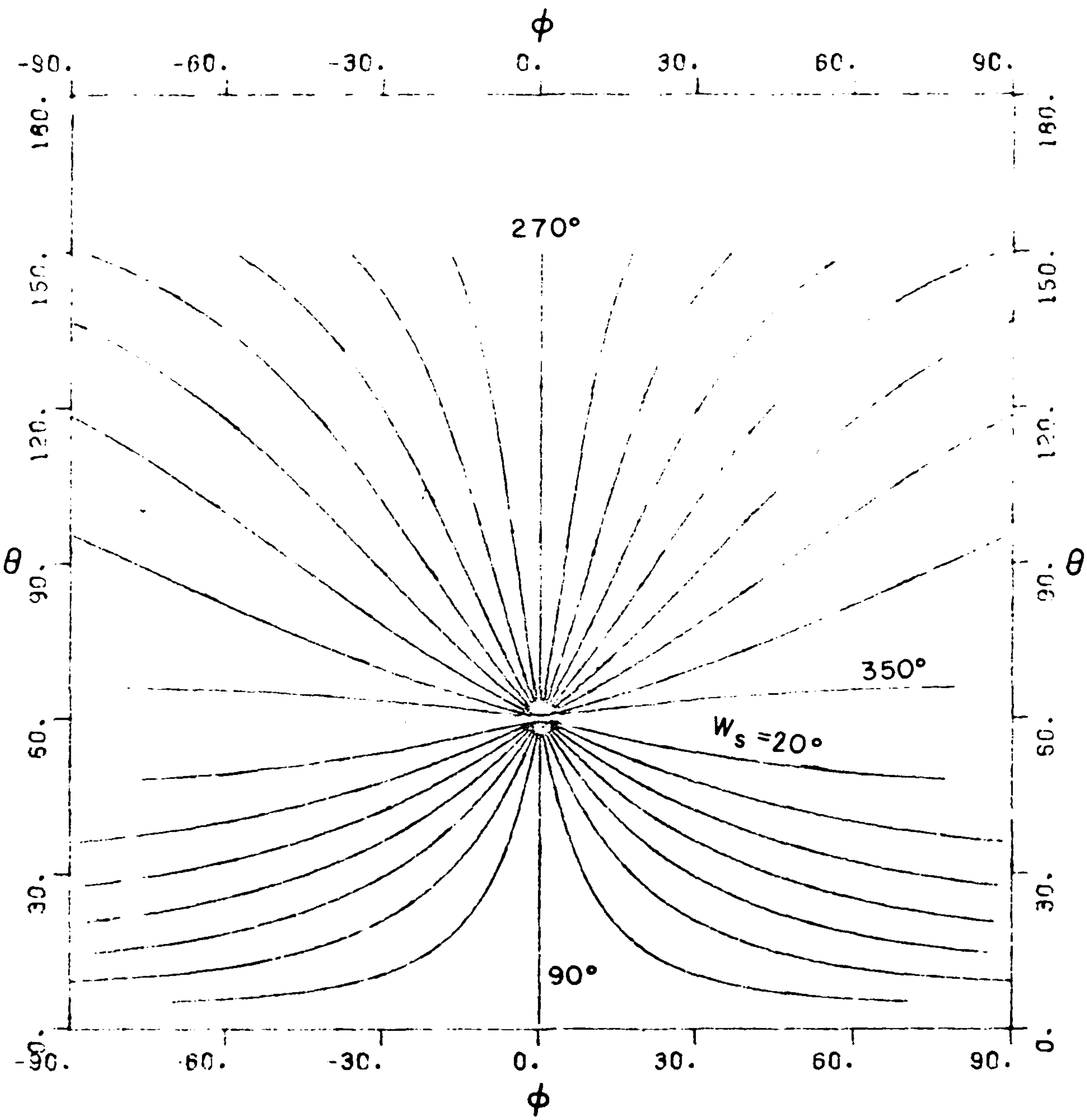

Figure 5. Geodesic paths on a 2x4 prolate spheroid. ($\theta_s=60^0,\phi_s=0^0$).

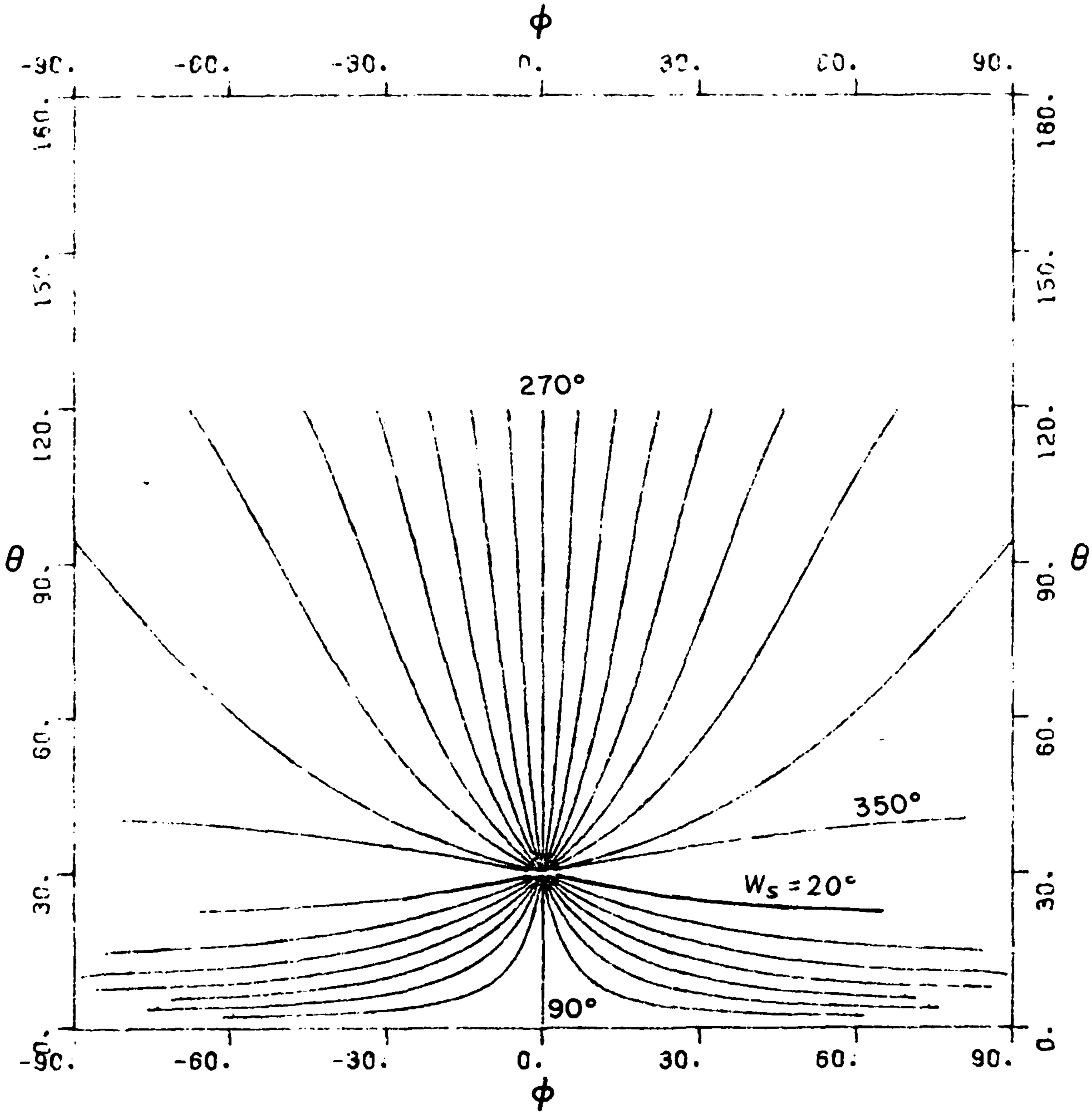

Figure 6. Geodesic paths on a 2x4 prolate spheroid. ($\theta_s=30^0, \phi_s=0^0$).

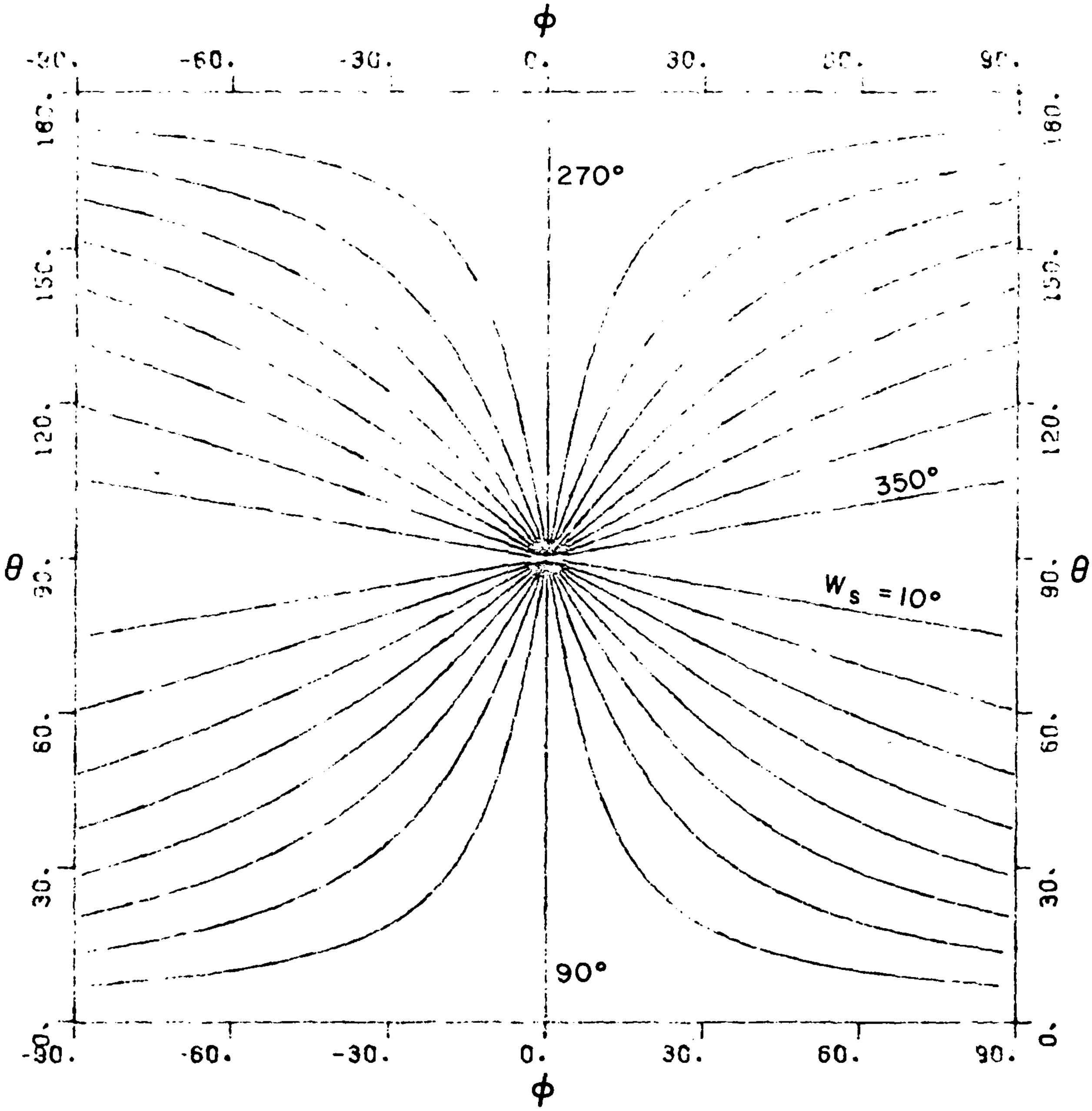

Figure 7. Geodesic paths on a 2x100 prolate spheroid. (θ_s=90^0, ϕ_s=0^0).

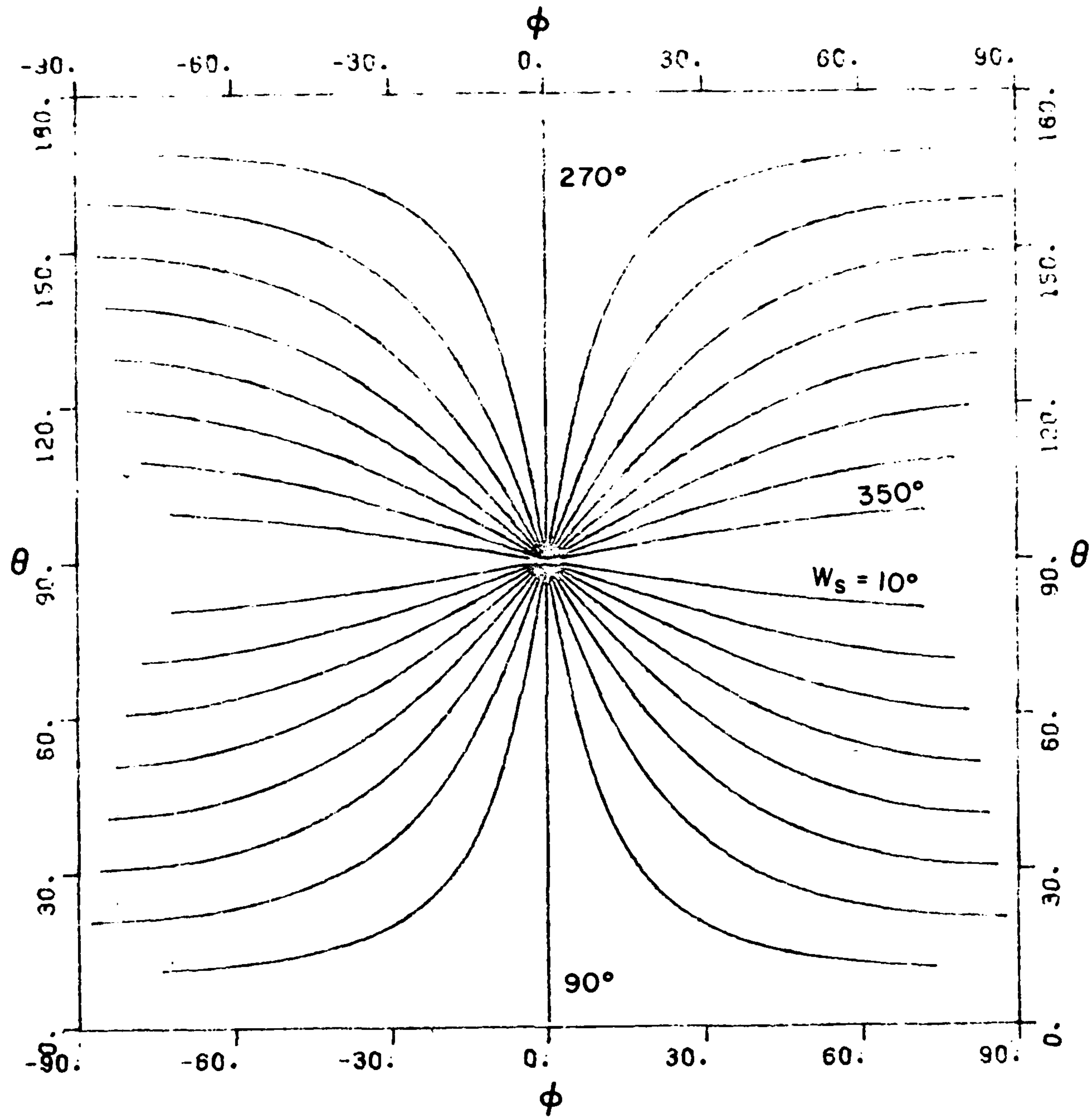

Figure 8. Geodesic path on a sphere. (θ_s=90^0,ϕ_s=0^0).

$$\vec{\gamma} = \begin{cases} R\sin\theta\cos\phi & \hat{x} \\ R\sin\theta\sin\phi & \hat{y} \\ R\cos\theta & \hat{z} \end{cases} \tag{8}$$

with

$$\phi = \phi_s + A\int_{\theta_s} \left[\frac{R'^2+R^2}{R'^2\sin^2\theta(R^2\sin^2\theta-A^2)} \right]^{1/2} d\theta \tag{9}$$

The unit tangent vector along the geodesic is

$$\hat{t} = \frac{d\overline{\gamma}}{d\ell} = \frac{d\overline{\gamma}}{d\theta}\bigg/\frac{d\ell}{d\theta} \ . \tag{10}$$

It can be shown that Equation (10) can be expressed as follows:

$$\hat{t} = t_x\hat{x} + t_y\hat{y} + t_z\hat{z} \tag{11}$$

where

$$t_x = \frac{\cos\phi(R'\sin\theta+R\cos\theta)-\phi'\sin\phi R\sin\theta}{D} \tag{12}$$

$$t_y = \frac{\sin\phi(R'\sin\theta+R\cos\theta)+\phi'\cos\phi R\sin\theta}{D} \tag{13}$$

$$t_z = \frac{R'\cos\theta-R\sin\theta}{D} \tag{14}$$

$$D = \frac{d\ell}{d\theta} = \text{sign}(\theta-\theta_s)\sqrt{R'^2+R^2+R^2\sin^2\theta(\phi')^2} \tag{15}$$

Note that ϕ' is given by Equation (4a).

It is convenient to express the tangent direction of the geodesic in terms of the spherical coordinate parameters θ_t and ϕ_t. From Equations (12), (13) and (14), the tangent direction angles θ_t and ϕ_t to the geodesic path can be determined as follows:

$$\theta_t = \cos^{-1}(t_z) \tag{16}$$

and

$$\phi_t = \tan^{-1}\left(\frac{t_y}{t_x}\right) \quad . \tag{17}$$

Numerical results for the tangent direction in terms of θ_t and ϕ_t for various geodesic curves are shown in Figs. 9, 10 and 11. It is interesting to observe that for the sphere case the geodesic tangent curves converge to one point, for the circular cylinder case these curves are parallel to each other, and finally for the prolate spheroid case, the tangent curves intersect each other in a caustic region. Once the unit tangent vector is determined, the other relevant parameter in the ray analysis, namely, the unit binormal vector $\hat{b}$ can readily be obtained via the equation $\hat{b} = \hat{t} \times \hat{n}$. The unit vector $\hat{n}$ is the outward normal vector of the surface.

Determination of the Geodesics on a Prolate Spheroid

In the proceeding section, a family of geodesic curves corresponding to a particular starting location on the surface of revolution has been determined. The associated tangent direction curves for each geodesic has also been found. According to the geometrical theory of diffraction, energy propagates outward from the source along the surface geodesic and continuously sheds electromagnetic energy in its tangent direction. Therefore, the next step is to determine the unique shedding point on a particular geodesic path at which the tangent points in the desired radiation direction. This task is performed in this section.

Consider now an antenna is located on a surface of revolution at S as shown in Fig. 1. The location parameters for the source point are (θ_s,ϕ_s). The desired radiation direction (θ_r,ϕ_r) is denoted with $\hat{r}$ which can be decomposed into its rectangular components as follows:

$$\hat{r} = r_x\hat{x} + r_y\hat{y} + r_z\hat{z} \quad . \tag{18}$$

where

$$r_x = \sin\theta_r\cos\phi_r \tag{19}$$

$$r_y = \sin\theta_r\sin\phi_r \tag{20}$$

$$r_z = \cos\theta_r \tag{21}$$

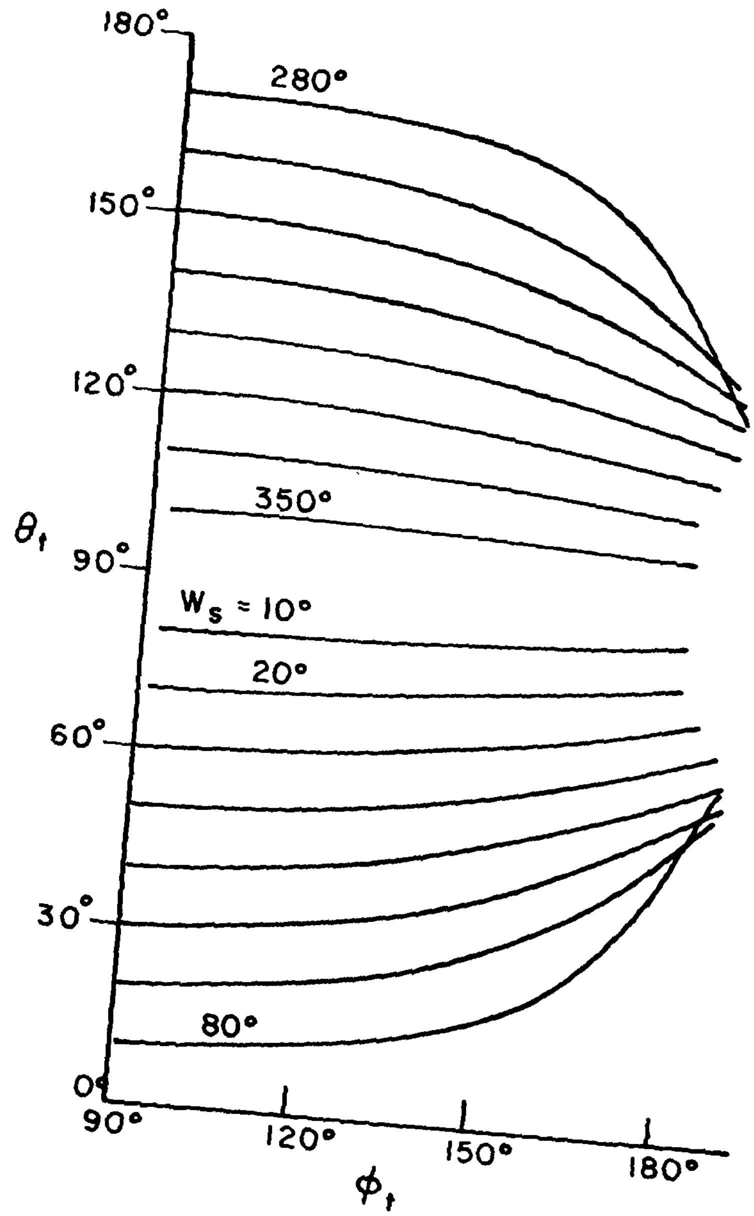

Figure 9. Tangent direction along the geodesic shown in Fig. 4.

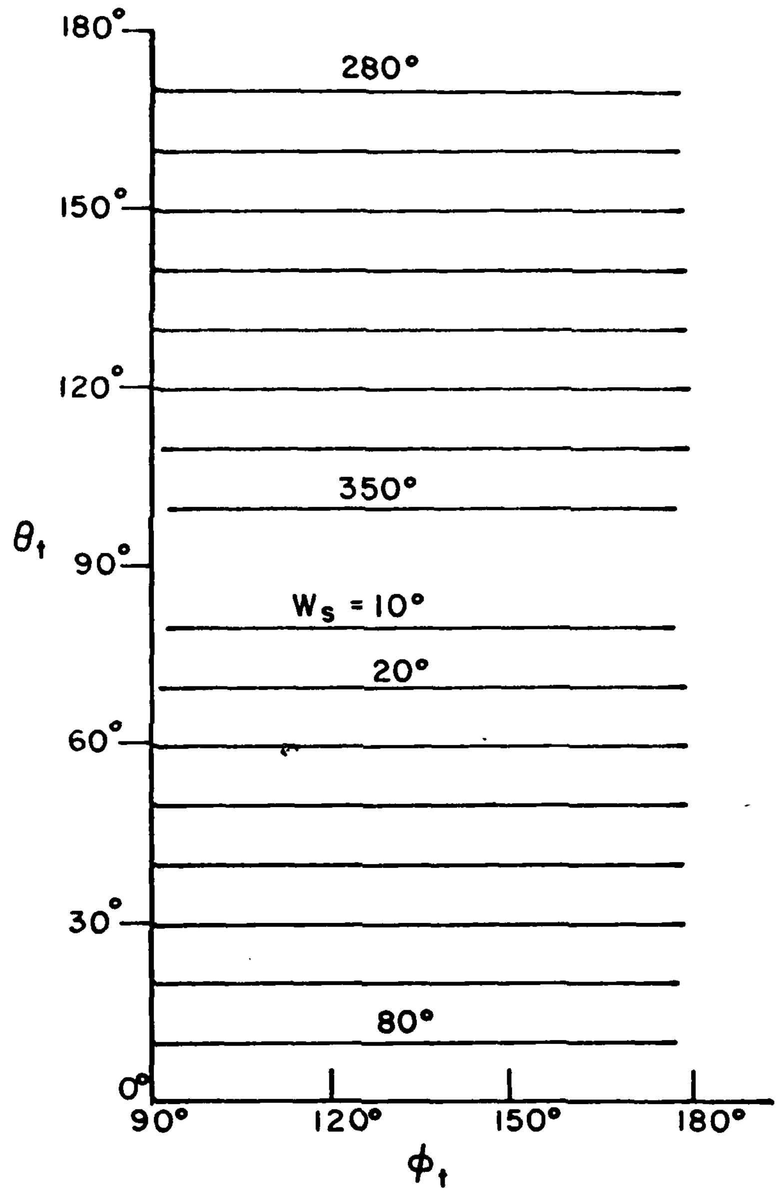

Figure 10. Tangent direction along the geodesic shown in Fig. 7.

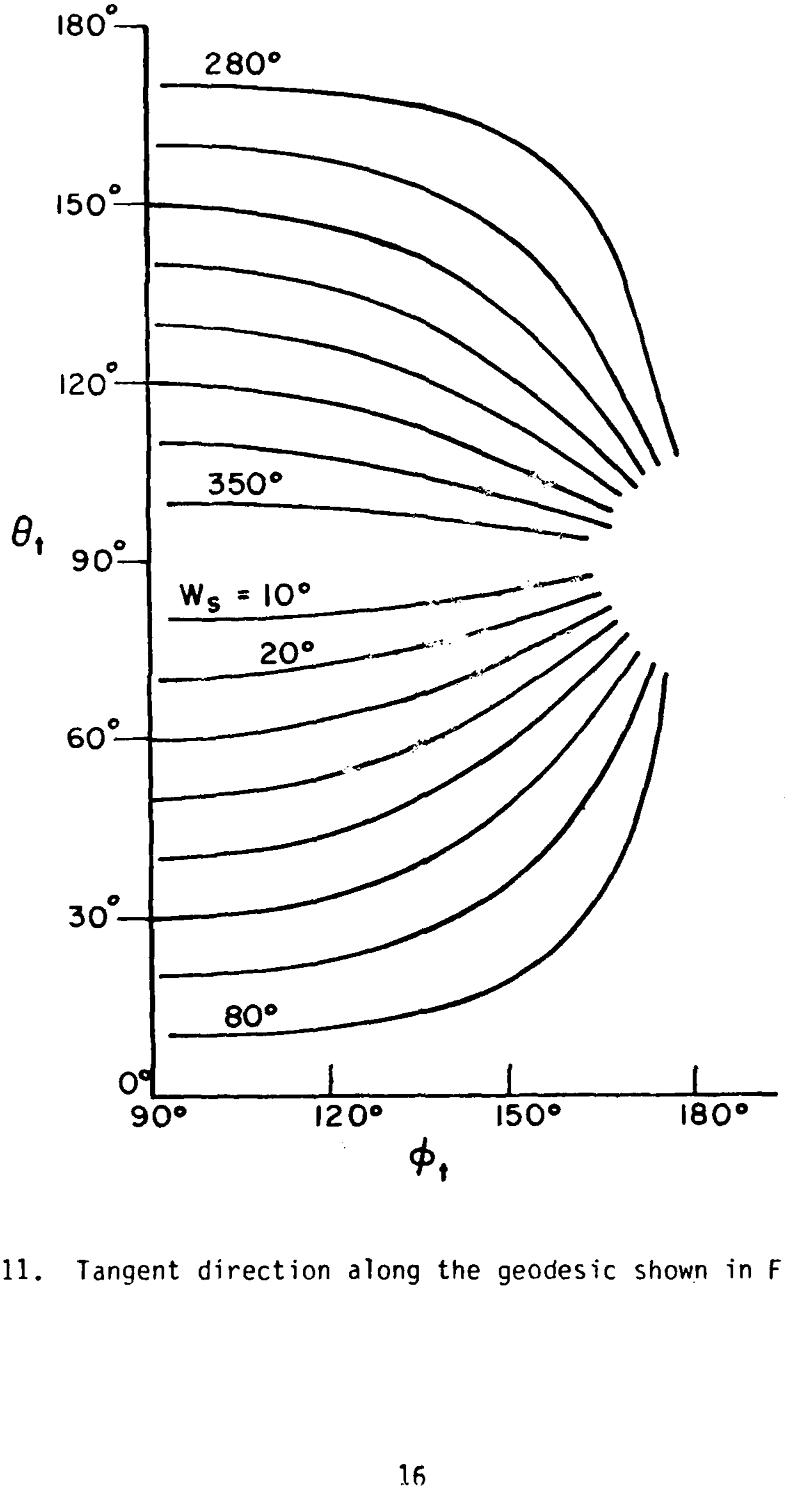

Figure 11. Tangent direction along the geodesic shown in Fig. 8.

Recall that the unit tangent vectors for the geodesic are given by Equations (11)-(15). Assuming at a particular point (θ_Q,ϕ_Q) on the surface of revolution, the tangent direction $\hat{t}|_Q$ matches with the radiation direction $\hat{r}$, then from Equations (11)-(15) and Equations (18)-(21) the following expressions are obtained:

$$\left.\frac{\cos\phi_Q(R'\sin\theta_Q+R\cos\theta_Q)-\sin\phi_Q R\sin\theta_Q\phi'}{D_Q}\right|_Q = \sin\theta_r\cos\phi_r \tag{22}$$

$$\left.\frac{\sin\phi_Q(R'\sin\theta_Q+R\cos\theta_Q)+\cos\phi_Q R\sin\theta_Q\phi'}{D_Q}\right|_Q = \sin\theta_r\sin\phi_r \tag{23}$$

and

$$\left.\frac{R'\cos\theta_Q-R\sin\theta_Q}{D_Q}\right|_Q = \cos\theta_r \tag{24}$$

where

$$D_Q = \mathrm{sign}(\theta_Q-\theta_S)\left.\sqrt{R'^2+R^2+R^2\sin^2\theta(\phi')^2}\right|_Q \tag{25}$$

and

$$\phi'|_Q = A_Q \left.\sqrt{\frac{R'^2+R^2}{R^2\sin^2\theta_Q(R^2\sin^2\theta_Q-A^2_Q)}}\right|_Q . \tag{26}$$

It is straightforward to show that from Equations (22)-(26) the following equations can be deduced:

$$A_Q = \mathrm{sign}(\theta_Q-\theta_S)R\sin\theta_Q\sin\theta_r\sin(\phi_r-\phi_Q)\Big|_Q \tag{27}$$

and

$$\phi_Q = \phi_r - \cos^{-1}\left(\frac{\cos\theta_r}{\sin\theta_r}\frac{R'\sin\theta_Q+R\cos\theta_Q}{R'\cos\theta_Q-R\sin\theta_Q}\right)\Bigg|_Q \tag{28}$$

In Equations (27) and (28), there are three unknowns θ_Q, ϕ_Q and A_Q and one needs one more equation to solve for the unknowns. This final equation is provided by the geodesic equation, Equation (4b), derived in Section II, namely,

$$\phi_Q = \phi_s + A_Q\int_{\theta_s}^{\theta_Q}\sqrt{\frac{R'^2+R^2}{R^2\sin^2\theta(R\sin^2\theta-A_Q^2)}}\,d\theta \quad . \tag{29}$$

From Equations (28) and (29) one obtains the following expression:

$$\phi_s + A_Q\int_{\theta_s}^{\theta_Q}\sqrt{\frac{R'^2+R^2}{R^2\sin^2\theta(R^2\sin^2\theta-A_Q^2)}}\,d\theta = \phi_r - \cos^{-1}\left[\frac{\cos\theta_Q}{\sin\theta_Q}\frac{R'\sin\theta_Q+R\cos\theta_Q}{R'\cos\theta_Q-R\sin\theta_Q}\right]\Bigg|_Q \quad . \tag{30}$$

Let us now proceed to eliminate A_Q from Equation (30). From Equation (28) one obtains the following equation:

$$\cos(\phi_r-\phi_Q) = \frac{\cos\theta_r}{\sin\theta_r}\left[\frac{R'\sin\theta_Q+R\cos\theta_Q}{R'\cos\theta_Q-R\sin\theta_Q}\right]\Bigg|_Q \quad . \tag{31}$$

Let us define

$$\cos\alpha \triangleq \cos(\phi_r-\phi_Q), \tag{32}$$

then from Equation (27), A_Q can be written as:

$$A_Q = \mathrm{sign}(\theta_Q - \theta_s) R \sin\theta_Q \sin\theta_r \sqrt{1-\cos^2\alpha}\,\Big|_Q \, . \qquad (33)$$

Note that $\cos\alpha$ is related to θ_Q via Equation (31) and Equation (32).

Finally, Equations (30) through (33) can be employed to determine the unique geodesic path and the unique diffraction point for a given source location on the surface of revolution and a given desired radiation direction. The secant method is suitable for solving the nonlinear equation, Equation (30). The initial points employed for the secant method are θ_s and θ_r where θ_r is given by Equation [illegible].

A simple and efficient computer program has been developed to solve the nonlinear equation, Equation (30) for the unknown θ_Q. The secant method with the initial points θ_s and θ_r, has been shown to be an extremely efficient and accurate method which converges in a few iteration steps. Once the θ_Q is determined, A_Q and ϕ_Q can be found via Equations (33) and the geodesic equation, Equation (28), respectively. Thus for a given source location (θ_s, ϕ_s), the unique geodesic path with a starting direction A_Q, and the unique diffraction point (θ_Q, ϕ_Q) on the surface of revolution that will radiate toward the desired radiation direction (θ_r, ϕ_r) has been found in an efficient manner.

Conclusion

A major task in the application of the geometrical theory of diffraction (GTD) to the problem of electromagnetic radiation from a general convex surface is to determine the unique geodesic path that starting from the source location traverses the surface and has a tangent at some point along the path which points in the desired radiation direction. In this report a numerically efficient and accurate scheme has been developed for solving this problem in the case of a general convex surface of revolution. The surface of revolution is of interest in that it provides an analytic model for the aircraft fuselage structure. A computer program is also developed to solve the governing nonlinear equation using the secant method for iteration. This method is proved to be simple and converges to the accurate results in just a few steps. Numerical results for the family of geodesic curves are also presented for the cases of sphere, prolate spheroid and cylinder.

REFERENCES

[1] W.D. Burnside, "Analysis of On-Aircraft Antenna Patterns," Report 3390-1, August 1972, The Ohio State University ElectroScience Laboratory, Department of Electrical Engineering; prepared under Contract No. N62269-72-C-0354 for Naval Air Development Center. (AD 777989)

[2] C.L. Yu and W.D. Burnside, "Volumetric Pattern Analysis of Fuselage Mounted Airborne Antennas," Report 2902-24, April 1976, The Ohio State University ElectroScience Laboratory, Department of Electrical Engineering; prepared under Grant No. NGL 36-008-138 for National Aeronautics and Space Administration, Washington, D.C. 20546.

[3] M.M. Lipschutz, Theory and Problems of Differential Geometry, Schaums Outline Series, McGraw-Hill Book Co., 1969.

[4] F.B. Hildebrand, Advanced Calculus for Applications, Prentice-Hall, New Jersey, 1962.